advances
in radiation oncology

Scientific Article

Prognostic Value of Early Fluorodeoxyglucose-Positron Emission Tomography Response Imaging and Peripheral Immunologic Biomarkers: Substudy of a Phase II Trial of Risk-Adaptive Chemoradiation for Unresectable Non-Small Cell Lung Cancer

Stephen R. Bowen, PhD,[a,b] Daniel S. Hippe, MS,[b] Hannah M. Thomas, PhD,[c] Balukrishna Sasidharan, MBBS, MD, DNB, DMRT,[c] Paul D. Lampe, PhD,[d] Christina S. Baik, MD, MPH,[e] Keith D. Eaton, MD, PhD,[e] Sylvia Lee, MD,[e] Renato G. Martins, MD, MPH,[e] Rafael Santana-Davila, MD,[e] Delphine L. Chen, MD,[b] Paul E. Kinahan, PhD,[b] Robert S. Miyaoka, PhD,[b] Hubert J. Vesselle, MD, PhD,[b] A. McGarry Houghton, MD,[d,f] Ramesh Rengan, MD, PhD,[a,f] and Jing Zeng, MD[a,*]

Departments of [a]Radiation Oncology and; [b]Radiology, University of Washington School of Medicine, Seattle, Washington; [c]Department of Radiation Oncology, Christian Medical College, Vellore, India; [d]Human Biology Division, Fred Hutchinson Cancer Research Center, Seattle, Washington; [e]Division of Medical Oncology, Department of Medicine, University of Washington School of Medicine, Seattle, Washington; [f]Clinical Research Division, Fred Hutchinson Cancer Research Center, Seattle, Washington

Abstract

Purpose: We sought to examine the prognostic value of fluorodeoxyglucose-positron emission tomography (PET) imaging during chemoradiation for unresectable non-small cell lung cancer for survival and hypothesized that tumor PET response is correlated with peripheral T-cell function.

Methods and Materials: Forty-five patients with American Joint Committee on Cancer version 7 stage IIB-IIIB non-small cell lung cancer enrolled in a phase II trial and received platinum-doublet chemotherapy concurrent with 6 weeks of radiation (NCT02773238). Fluorodeoxyglucose-PET was performed before treatment start and after 24 Gy of radiation (week 3). PET response status was prospectively defined by multifactorial radiologic interpretation. PET responders received 60 Gy in 30 fractions, while nonresponders received concomitant boosts to 74 Gy in 30 fractions. Peripheral blood was drawn synchronously with PET imaging, from which germline DNA sequencing, T-cell receptor sequencing, and plasma cytokine analysis were performed.

Results: Median follow-up was 18.8 months, 1-year overall survival (OS) 82%, 1-year progression-free survival 53%, and 1-year locoregional control 88%. Higher midtreatment PET total lesion glycolysis was detrimental to OS (1 year 87% vs 63%, $P < .001$), progression-free survival (1 year 60% vs 26%, $P = .044$), and locoregional control (1 year 94% vs 65%, $P = .012$), even after adjustment for clinical/treatment factors. Twenty-nine of 45 patients (64%) were classified as PET responders based on a priori definition. Higher tumor programmed death-ligand 1 expression was correlated with response on PET ($P = .017$). Higher T-cell receptor richness and clone distribution slope were associated with improved OS ($P = .018-0.035$); clone distribution slope was correlated with PET response ($P = .031$).

Conclusions: Midchemoradiation PET imaging is prognostic for survival; PET response may be linked to tumor and peripheral T-cell biomarkers.

Introduction

The current standard of care for locally advanced, unresectable non-small cell lung cancer (NSCLC) is concurrent chemoradiation plus a year of adjuvant durvalumab, a programmed death-ligand 1 (PD-L1) immune checkpoint inhibitor, which improved survival over chemoradiation alone per the PACIFIC trial.[1,2] However, patient outcomes remain suboptimal even for well-selected clinical trial-eligible patients, with an overall survival (OS) at 2 years of 66.3%.[1] Clinical trials seek to improve outcomes through intensification of therapy, both in terms of additional immune-modulating therapy as well as localized radiation dose escalation. Beyond durvalumab, other checkpoint inhibitors are also being tested as consolidation therapy after chemoradiation, concurrent with chemoradiation, and neoadjuvant to chemoradiation.[3] As treatment intensifies, patient tolerance is increasingly challenged, with 29.1% of patients experiencing serious adverse events in the PACIFIC trial and 15.4% of patients discontinuing treatment due to adverse events. Although durvalumab improved 3-year OS from 44.1% to 56.5% in the PACIFIC trial, only a subset of the patients who received durvalumab derived a survival benefit from the additional treatment (ie, 44.1% of patients were alive at 3 years without durvalumab).[4] A prognostic test that could predict patient outcome would help better select patients who need additional therapies, and spare toxicity in patients who do not.

Fluorodeoxyglucose-positron emission tomography (FDG-PET) imaging during chemoradiation for NSCLC has been correlated with treatment response and survival.[5-9] Van Elmpt et al[10] found that for patients whose mean tumor standardized uptake values (SUV) decreased by >15% on midtreatment PET, 2-year OS was 92% compared with 33% for patients with a decrease in mean SUV <15%. Tumor FDG-PET avidity has also been correlated with PD-L1 expression, with multiple clinical series suggesting SUV_{max} may be associated with PD-L1 positivity and that SUV_{max} could be a potential predictive marker of response to anti-PD-1 therapy in patients with NSCLC.[11,12]

In addition to predicting for survival, FDG-PET avidity may also be predictive for local recurrences,[13,14] both on the prechemoradiation scan and the midchemoradiation scan. Decades of trials to overcome local recurrence risk by radiation treatment intensification in unresectable NSCLC have yielded limited success. Results of Radiation Therapy Oncology Group (RTOG) 0617 showing inferior outcomes with 74 versus 60 Gy during concurrent chemoradiation were unexpected, and 60 Gy continues to be the standard of care radiation dose.[15] However, local control remains a problem in stage III NSCLC, with locoregional failures of around 20% to 30% by 2 years and rising to 50% by 3 to 5 years.[1,16-18] There are multiple hypotheses as to lack of benefit with 74 versus 60 Gy in RTOG 0617. Higher radiation dose to normal tissues such as the heart was highly correlated with survival, as well as the degree of esophagitis experienced during treatment.[15] Because dose escalation for all patients with locally advanced NSCLC seems harmful, many clinical trials are testing other strategies for dose escalation. Some trials have tested giving all patients a radiation boost based on pretreatment PET scans, targeting the most FDG-avid regions with a higher dose of radiation,[19,20] whereas other trials dose-escalate all patients based on midtreatment PET.[21] Because some patients are cured with 60 Gy of radiation, not everyone benefits from dose escalation. We designed a phase II trial FLARE-RT (NCT02773238) where select patients undergo dose escalation based on midtreatment FDG-PET response, and only nonresponders undergo dose escalation (74 Gy) for the second half of chemoradiation.[22]

We investigated whether early FDG-PET response imaging during chemoradiation has prognostic value in patients treated in the FLARE-RT trial, and hypothesized that a robust tumor PET response is linked to peripheral T-cell function, given the clinical and preclinical data that a robust tumor response to radiation requires an intact immune system, including the presence of CD8+ T-cells.[23,24] The purpose of this biomarker substudy under the parent clinical trial was to (1) evaluate the prognostic value of previously reported FDG-PET imaging biomarkers during chemoradiation; (2) evaluate peripheral immunologic biomarkers and correlates of PET imaging; and (3) identify complementary markers of tumor biology (PET response) and disease burden (total lesion glycolysis). Biomarkers of early treatment response/resistance can support clinical management decisions and inform the design of next-generation
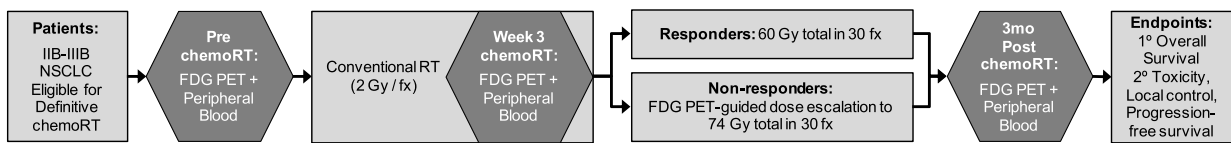
Fig. 1 FLARE-RT phase II trial schema of risk-adaptive chemoradiation for patients with unresectable locally advanced non-small cell lung cancer.

biomarker-guided and risk-adaptive clinical trials to improve outcomes in patients with LA-NSCLC.

Methods and Materials

Clinical trial protocol

The FLARE-RT phase II trial (NCT02773238) schema is shown in Figure 1. This research was institutional review board approved and conducted in accord with the ethical standards of our institution. Patients with histopathologically confirmed unresectable American Joint Committee on Cancer v7 stage IIB-IIIB NSCLC and Eastern Cooperative Oncology Group performance status 0 to 1 were enrolled from 2016 to 2020. Baseline FDG-PET imaging was followed by initiation of definitive chemoradiation planned for 60 Gy in 30 fractions. Chemotherapy consisted of a platinum doublet per physician choice (Table 1) and started at the same time as radiation. Consolidation immunotherapy was allowed postchemoradiation once it became standard of care. During the third week of chemoradiation (after 24 Gy delivered), FDG-PET imaging was performed to assess early treatment response. Patients prospectively classified as responders continued to receive a total dose of 60 Gy in 30 fractions, while those classified as nonresponders received a concomitant dose boost over the final 15 fractions (2.93 Gy daily) to a total dose of 74 Gy in 30 fractions, as previously described.[22] The precision dose boost was spatially localized and redistributed to conform to residual intratumoral FDG avidity. All standard normal tissue dose constraints were followed per protocol. Peripheral blood draws were completed synchronously with PET imaging at baseline, week 3 midtreatment, and 3-month posttreatment time points. The primary trial endpoint was 2-year OS, while secondary endpoints included 1-year progression-free survival (PFS), 1-year locoregional control (LRC), and pulmonary toxicity (Common Terminology Criteria for Adverse Events v4 grade 2 + pneumonitis).

PET response assessment and PET biomarker definition

Week 3 PET response status was prospectively defined by multifactorial radiologic interpretation for selective treatment adaptation. Interval changes in SUV metrics (SUV_{max}, SUV_{mean}, SUV_{peak}), metabolic tumor volume (MTV), and total lesion glycolysis (TLG) were used to prospectively score PET response using semiautomatic gradient-based segmentation of the primary tumor and adjacent involved lymph nodes. PET responders were predefined as patients with greater than 20% decrease in at least 1 metric of FDG avidity (SUV_{max}, SUV_{mean}, SUV_{peak}) and at least 1 metric of FDG volumetric extent (MTV, TLG). MTVs were delineated by a commercially validated segmentation algorithm (PET Edge; MIM Software, Cleveland, OH) that achieved improved interobserver agreement compared with manual contouring and reduced sensitivity to image reconstruction compared with fixed threshold contouring.[25,26] Protocol-defined midchemoradiation PET response status showed substantial agreement with retrospective midchemoradiation PET response assessment by positron emission tomography response criteria in solid tumors (PERCIST) 1.0 (kappa, 0.72 [0.51-0.93]).[27,28]

Beyond week 3 PET response status as a single binary variable, we restricted prognostic evaluation of week 3 PET biomarkers to total lesion glycolysis (TLG_{midtx} [g]), representing metabolic disease burden and the product of MTV (mL) with SUV_{mean} (g/mL).[4,9,29] Given the skewed distribution of TLG_{midtx} across patients, we dichotomized the upper tail of the distribution from the bulk, which was achieved at the 80th percentile and corresponding threshold of TLG_{midtx} = 250 g. TLG_{midtx} defined risk strata in univariable survival analysis for OS, PFS, and LRC endpoints. TLG_{midtx} multivariable survival analyses consisted of individual effect size adjustments for baseline TLG_{pretx}, clinical factors (age, histology, PD-L1 expression, driver mutation presence), and treatment factors (radiation modality, consolidation immunotherapy, radiation target volume).

Peripheral blood genomic and immunologic assays

Sequencing of peripheral germline DNA was conducted using the Infinium Global Screening Array (Illumina Inc, San Diego, CA), which included sample quality control (QC), library prep + QC, cluster optimization, and sequencing steps. Sequencing libraries were prepared with a Covaris LE220 system and PerkinElmer Sciclone

Table 1   Patient characteristics (N = 45)

Characteristic	n (%) or median (range)
Age (years)	63 (34-78)
Gender	
Female	25 (56%)
Male	20 (44%)
Histology	
Adenocarcinoma	29 (64%)
Squamous cell carcinoma	14 (31%)
Other	2 (4%)
Chemotherapy	
Carboplatin-paclitaxel	25 (56%)
Cisplatin-etoposide	11 (24%)
Other platinum doublet	9 (20%)
Stage (AJCC v7)	
IIB	2 (4%)
IIIA	23 (51%)
IIIB	15 (33%)
N2 recurrence	5 (11%)
Radiation therapy	
Photon IMRT	22 (49%)
Proton beam radiation	23 (51%)
Consolidation immune checkpoint inhibitor	
Yes	23 (51%)
No	22 (49%)
PD-L1 tumor proportion score	
>50%	6 (13%)
1%-49%	7 (16%)
<1%	7 (16%)
Unknown	25 (56%)
Driver mutation (*EGFR/ALK/ROS1*)	
Yes	9 (20%)
No	19 (42%)
Unknown	17 (38%)
Mid-PET response	
Responder	29 (64%)
Nonresponder	16 (36%)
Mid-PET PERCIST 1.0	
Partial metabolic responder	27 (60%)
Stable metabolic disease	17 (38%)
Progressive metabolic disease	1 (2%)

Abbreviations: AJCC = American Joint Committee on Cancer; *ALK* = anaplastic lymphoma kinase; *EGFR* = epidermal growth factor receptor; IMRT = intensity modulated radiation therapy; PD-L1 = programmed death-ligand 1; PERCIST = positron emission tomography response criteria in solid tumors; PET = positron emission tomography; *ROS1* = c-ros oncogene 1.

NGSx workstation. Library QC was ensured with 2 Agilent Bioanalyzer 2100, an Agilent 2200 TapeStation, a Life Technologies Qubit 2.0 fluorometer, and an ABI StepOne Real-Time PCR system. Genotypes with GenCall scores >0.15 were considered sufficient quality for inclusion. Genome sequencing reports were filtered to include single nucleotide polymorphism (SNP) genotypes from a list of predefined relevant candidate genes (see Table E1) belonging to different pathway families: 96 DNA repair genes,[23,30] 53 immunology genes,[31-33] 38 oncology genes,[34,35] and 27 lung biology genes.[36]

Molecular T-cell receptor (TCR) β chain CDR3 sequencing was carried out on the ImmunoSEQ platform (Adaptive Biotechnologies, Snohomish, WA) with a survey sampling depth of 120,000 T-cells. TCR richness was averaged over the following measures due to high collinearity (Spearman r > 0.93): iChao1,[37] Efron Thisted estimator,[38] and Daley Smith estimator.[39] Clonality/evenness measures included the following: Pielou evenness,[40] Simpson clonality and evenness,[29] and clone distribution slope.[41]

Exploratory single immune cell functional assays were performed using IsoCode Human Adaptive Immune chips (Isoplexis, Branford, CT), which measure 25 + cytokine secretions on a single cell base of approximately 1000 individual cells per chip. We restricted our analysis to polyfunctional CD8+ T-cells, following stimulation and secretion of at least 2 effector cytokines. Lastly, detectable plasma concentrations from an immunologic panel of 43 cytokines were measured via a combination of the Luminex200 microbead system (Luminex, Austin, TX) and standard enzyme-linked immunosorbent assay.

Statistical analysis

OS, PFS, and distant metastatic-free survival rates were estimated by Kaplan-Meier. LRC and pneumonitis (PNM) rates were adjusted for distant progression and death as competing risks. Differences between risk strata were evaluated with log rank or Gray's testing. Univariable and multivariable hazard ratios (HR) were estimated by Cox regression or Fine and Gray competing risk regression. Hierarchical clustering of peripheral germline DNA sequencing SNP genotypes was performed and summarized with cumulative frequency distributions of rank-ordered SNPs for each genetic pathway family (DNA repair, immunology, oncology, lung biology). Genotype associations with PET response status, survival outcomes, and TLG_{midtx} were characterized by logistic regression with Firth penalization, Cox regression with Firth penalization, and Spearman rank correlation, as appropriate. PD-L1 tumor proportion score (TPS) associations to PET response status, TLG_{midtx}, and clinical factors were summarized by logistic regression with Firth penalization, Spearman rank correlation, and Fisher exact testing, as appropriate. TCR diversity metric trends over

pretreatment, midtreatment, and posttreatment time-points were estimated by Spearman rank correlation and pairwise changes by Wilcoxon signed rank testing. TCR diversity metric associations to OS and PFS were assessed by permutation testing of Harrell's c-index, while TCR diversity metric associations to PET response class and TLG_{midtx} were assessed by groupwise Wilcoxon rank sum testing and Spearman rank correlation, as appropriate. Hierarchical clustering of plasma cytokines was performed and summarized with a 2-dimensional dendrogram heatmap of cytokine concentration z scores with rugs for OS, PFS, PET response, and TLG_{midtx} classes. Associations of cytokines with PET response status, survival outcomes, and TLG_{midtx} were assessed by Fisher exact testing, Cox regression with Firth penalization, and Spearman rank correlation, as appropriate. All statistical analyses and data visualization were carried out in Origin-Pro 2020b (OriginLab, Northampton, MA) and R version 4.0.3 (R Statistical Language, Vienna, Austria). Throughout, 2-sided tests were used with $P < .05$ considered statistically significant, without adjustment for the number of comparisons across prespecified imaging and peripheral immunologic biomarkers.

Results

Patient characteristics

Patient characteristics are summarized in Table 1. Forty-nine patients were enrolled but 4 patients did not initiate any clinical trial therapy (3 were found to have metastatic disease on repeat baseline imaging, and 1 patient chose to have surgery instead). In the intention-to-treat population (n = 45) with median age of 63 years (range, 34-78 years), most patients enrolled in the trial had unresectable, stage III, multistation N2 positive NSCLC. Approximately half of the patients received consolidation immune checkpoint inhibitor therapy when the standard of care changed midpoint during this trial (Table 1), and about half of the patients were treated with proton beam radiation (Table 1) and half with photon intensity modulated radiation therapy. Twenty-nine of 45 patients (64%) were prospectively classified as PET responders per protocol definition.

Clinical outcomes

Figure 2 summarizes clinical outcomes of the phase II trial from the time of consent. The median time between consent and start of chemoradiation was 11 days (range, 0-24 days). After a median follow-up of 18.8 months (range, 3.0-49.9 months), 1-year OS was 82%, 1-year PFS was 53%, 1-year LRC was 88%, 1-year distant metastatic-free survival was 61%, and 6-month PNM cumulative incidence was 25%. Two of 45 patients terminated chemoradiation early due to progressive disease during chemoradiation and switched to systemic therapy alone but were included in the analysis. Patients who received durvalumab had numerically higher cumulative incidence of grade 2 + PNM versus those who did not, though the difference was not statistically significant (1-year PNM 52% vs 26%, Gray $P = .20$). Receipt of consolidation durvalumab according to the PACIFIC regimen resulted in numerically higher PFS but did not reach statistical significance in our trial cohort (median PFS 19.4 vs 10.9 months, log rank $P = .45$).

Week 3 midtreatment PET risk stratification

PET response status, representing midtreatment interval changes in imaging biomarkers and the basis for adaptive radiation dose escalation in select patients, was not associated with OS (log rank $P = .63$), PFS (log rank $P = .62$), and LRC (Gray $P = .25$). Figure 3A-C shows that larger residual TLG_{midtx} on week 3 PET, dichotomized at the 80th percentile (250 g), was significantly associated with a detriment in OS (log rank $P < .001$), PFS (log rank $P = .044$), and LRC (Gray $P = .012$). Figure 3D captures a possible association between PET response status and TLG_{midtx} that modulated PFS (log rank $P < .00001$), in which the highest risk of rapid disease progression was in PET nonresponders with $TLG_{midtx} > 250$ g. Of the 9 patients with $TLG_{midtx} > 250$ g, 6/9 were classified as PET responders and received standard chemoradiation without PET-guided dose escalation. Given the modest sample size, a formal interaction test between PET response and TLG_{midtx} was not performed. Forest plots summarize the univariable associations of TLG_{midtx} with OS (Fig 3E) or PFS (Fig 3F) as well as multivariable associations of TLG_{midtx} with OS (Fig 3E) or PFS (Fig 3F) after individual adjustment of relevant factors, including radiation target volume (PTV_{pretx}), baseline metabolic disease burden (TLG_{pretx}), and PET response status. TLG_{midtx} was independently prognostic for PFS following all adjustments, and independently prognostic for OS with the exception of TLG_{pretx} adjustment. In this case, TLG_{midtx} had a relatively larger effect size on OS compared with TLG_{pretx} (HR 1.65 vs HR 1.00, $P = .15$).

Peripheral germline DNA sequencing

Figure 4 depicts the cumulative frequency of SNP genotypes of different genetic pathway families (DNA repair, immunology, lung biology, oncology) in 19 patients rank ordered by their effect size on unsupervised hierarchical cluster membership (A), risk of death (B), PET response class membership (C), and residual total lesion glycolysis
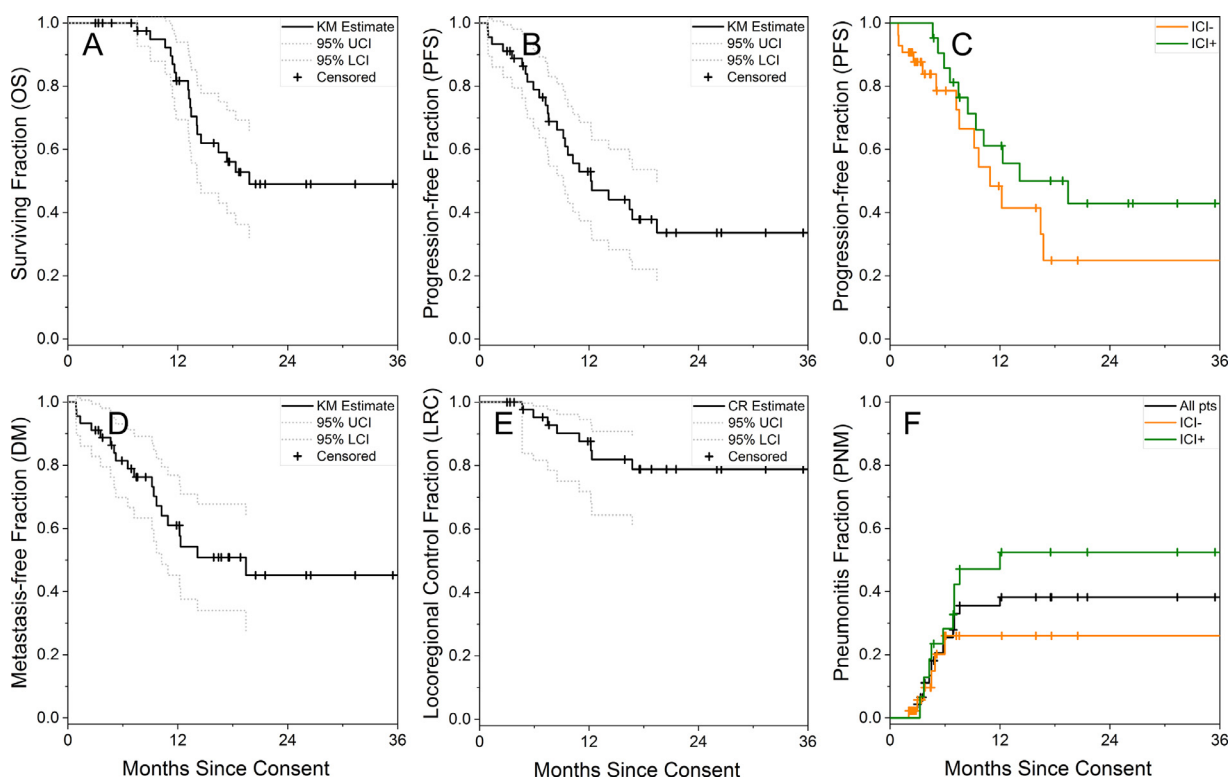
Fig. 2 FLARE-RT clinical trial outcomes: OS **(A)**, PFS **(B)**, PFS stratified by receipt of consolidation ICI **(C)**, DM **(D)**, LRC **(E)**, CTCAE v4 grade 2 or higher PNM **(F)**. *Abbreviations:* CR = competing risk (distant progression/death); CTCAE = Common Terminology Criteria for Adverse Events; DM = distant metastatic-free survival; ICI = immune checkpoint inhibitor therapy; KM = Kaplan-Meier; LRC = locoregional control; OS = overall survival; PFS = progression-free survival; PNM = pneumonitis.

correlation (D). A larger frequency of SNP gene alterations in the immunology pathways belonged to the main hierarchical cluster and had significant association with OS (Fig 4A,B) relative to other pathway families that resided closer to the diagonal reference line of equal frequency contribution. Differences in gene alteration frequency between PET nonresponder and responder subgroups were observed across several pathway families, particularly immunology and oncology (Fig 4C). By contrast, there was no preferential correlation of specific pathway families with TLG_{midtx}, which all had cumulative frequency distributions that closely followed the diagonal reference line (Fig 4D). Of the top 30 SNPs ranked by association with PET response status ($P < .016$), a plurality (13/30) came from immunologic pathways, while none of these same SNPs were associated with total lesion glycolysis ($P > .11$). Immunologic pathway genetic differences in *JAK1* associated with PET response status and PFS ($P = .033-.040$), while differences in *STAT1* ($P = .001-.030$) and interferon gamma (*IFNγ*) ($P = .002-.060$) associated with PET response status and hierarchical cluster membership. Other associations with PET response status included germline genetic alterations in vascular endothelial growth factor C (*VEGFC*) ($P = .002$), anaplastic

lymphoma kinase (*ALK*) ($P = .018$), and epidermal growth factor receptor (*EGFR*) ($P = .047$). Associations with OS included immuno-oncogene alterations in *ALK* ($P = .012$), *PIK3CA* ($P = .013$), and tumor necrosis factor (*TNF*) ($P = .041$). None of these gene alterations were associated with TLG_{midtx} ($P > .38$). Without adjustments for multiple comparisons, our results are hypothesis generating and require definitive independent validation.

PET response versus tumor PD-L1 expression

PET response status was correlated with PD-L1 TPS in 20 patients: 6/6 patients with high PD-L1 TPS (≥50%) were PET responders and 6/7 with moderate PD-L1 TPS (1%-49%) were PET responders. By contrast, 4/5 patients classified as PET nonresponders had PD-L1 TPS <1%. The association between PET response and PD-L1 TPS was statistically significant as a trend across 3 expression levels (<1%, 1%-49%, ≥50%, Firth $P = .017$), rank correlation (Spearman $r = 0.54$, $P = .014$), and categorical frequency (<1% vs ≥1%, Fisher $P = .031$). The association with PET response status was not confounded by availability of PD-L1 testing results: 15/20 were PET
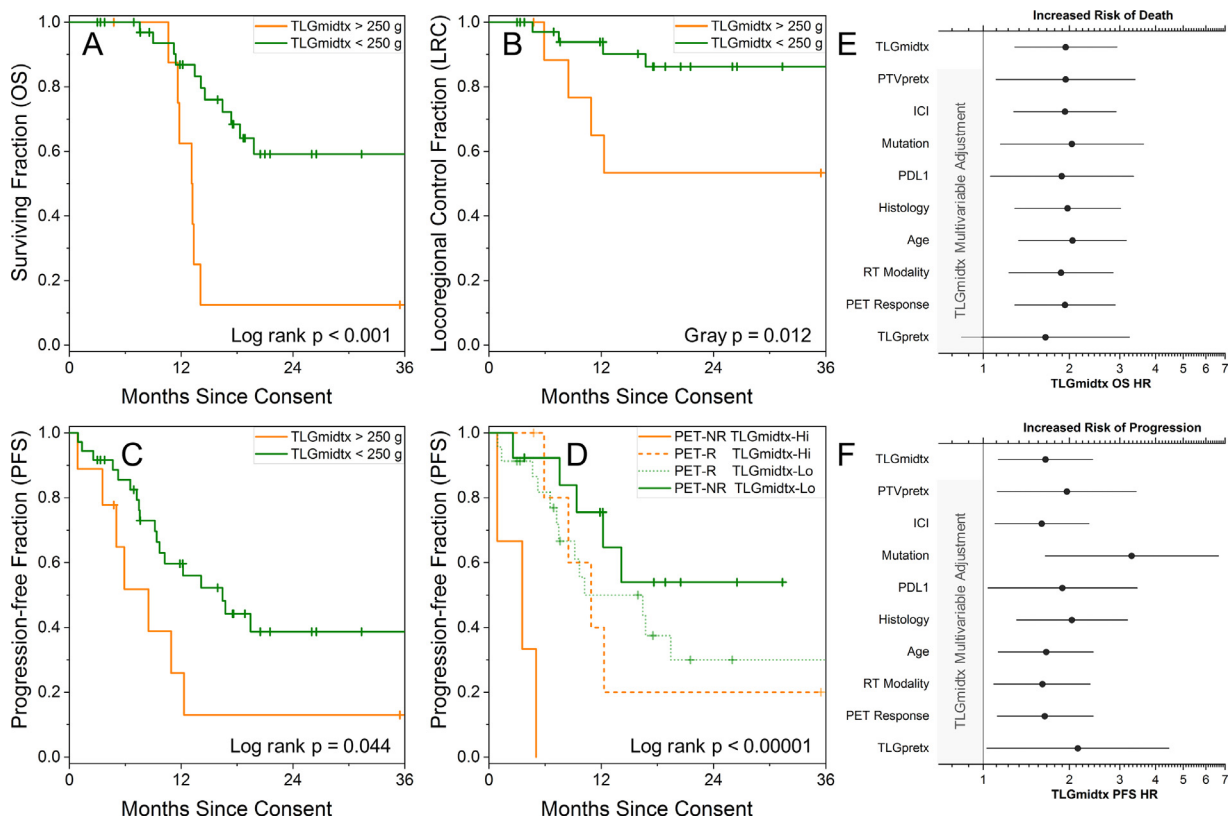
Fig. 3 Kaplan-Meier OS, competing risk-adjusted LRC, and Kaplan-Meier PFS stratified by week 3 midtreatment FDG-PET total lesion glycolysis (TLG$_{midtx}$) **(A-C)**, along with association of total lesion glycolysis with PET response status for PFS **(D)**. Forest plots of total lesion glycolysis OS and PFS univariate and bivariate hazard ratios, adjusted for individual clinical and treatment factors **(E,F)**. *Abbreviations:* FDG-PET = fluorodeoxyglucose-positron emission tomography; LRC = locoregional control; OS = overall survival; PET-NR = PET nonresponder; PET-R = PET responder; PFS = progression-free survival.

responders when PD-L1 was available compared with 14/25 PET responders when unavailable (Fisher *P* = .22). Tumor PD-L1 expression was neither correlated with midtreatment total lesion glycolysis (Spearman r = 0.04, *P* = .88) nor associated with histology, stage, or presence of a driver mutation (*P* > .28).

TCR diversity metrics and CD8+ T-cell polyfunctionality

TCR sequencing was performed at pretreatment (n = 15), midtreatment (n = 15), and 3-months posttreatment (n = 10) time points. No patients received immunotherapy prechemoradiation treatment or midtreatment, and 10/10 patients were receiving immunotherapy (durvalumab) at the posttreatment time point. TCR average richness declined significantly across time points (Fig 5A, *P* = .001). Pairwise changes were most significant between pre- and posttreatment time points (Wilcoxon signed rank *P* = .037). Higher pretreatment TCR richness (Fig 5B, permutation *P* = .018), higher pretreatment clone

distribution slope (Fig 5D, permutation *P* = .035), and smaller decline in clone distribution slope (permutation *P* = .050) were associated with improved OS. Pretreatment TCR clone distribution slope, pre- and midtreatment clonality, and midtreatment evenness were correlated with PET response status (Wilcoxon rank-sum *P* = .031-.048). None of the TCR diversity metrics were strongly correlated with midtreatment TLG$_{midtx}$ (median Spearman |r| = 0.17 [0.04-0.52]). Patients classified as midtreatment PET responders had higher percentage of peripheral polyfunctional CD8+ T-cells compared with midtreatment PET nonresponders (Fig 5C, 0.7%-1.3% vs 0%-0.1% expressing MIP1b and IFNγ). There was no association between TLG$_{midtx}$ and peripheral CD8+ T-cell functionality.

Plasma cytokine levels

Figure E1 displays the midtreatment peripheral blood plasma cytokine hierarchical clustering dendrogram with heatmap scaled by z scores of cytokine concentration levels and rugs for OS, PFS, and PET response status. While
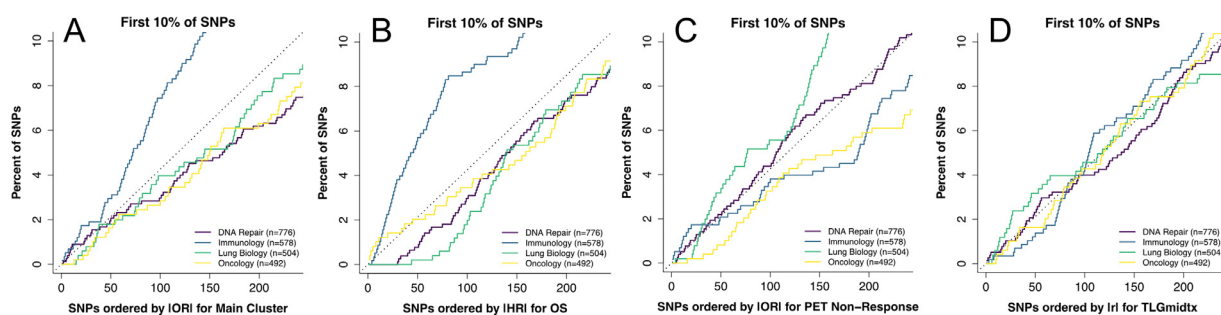
Fig. 4 Peripheral DNA microarray cumulative frequency distribution of SNP gene alterations by pathways (DNA repair, immunology, lung biology, oncology). The SNPs are ordered based on **(A)** OR for membership in unsupervised hierarchical clusters, **(B)** HR for OS endpoint, **(C)** OR for PET nonresponder group, and **(D)** Spearman correlation (r) to PET total lesion glycolysis (TLG_midtx). The diagonal reference line represents equal frequency contributions from all SNPs across pathways. Immunologic pathway gene alteration frequency has an outsized effect on risk of death (B, blue curve) relative to other pathways. PET response status shows highly significant association to gene alterations across several pathways (C, blue, yellow, green curves), while PET TLG_midtx correlations to gene alterations are more randomly distributed near the diagonal reference line without linkages to specific pathways (D). *Abbreviations:* HR = hazard ratio; OR = odds ratio; OS = overall survival; PET = positron emission tomography; r = Spearman rank correlation; SNP = single nucleotide polymorphism.

the 23 patients were not distinctly clustered by cytokine levels, hierarchical clusters of cytokines included the following: (1) MIP1b, IFNγ, TNFR1, TNFR2, TNFα; (2) VEGF, TGFb1. Among these select cytokines, the only significant correlation we identified was that lower midtreatment TNFR1 plasma concentration relative to baseline plasma concentration was associated with worse PFS (HR 0.43, P = .005).
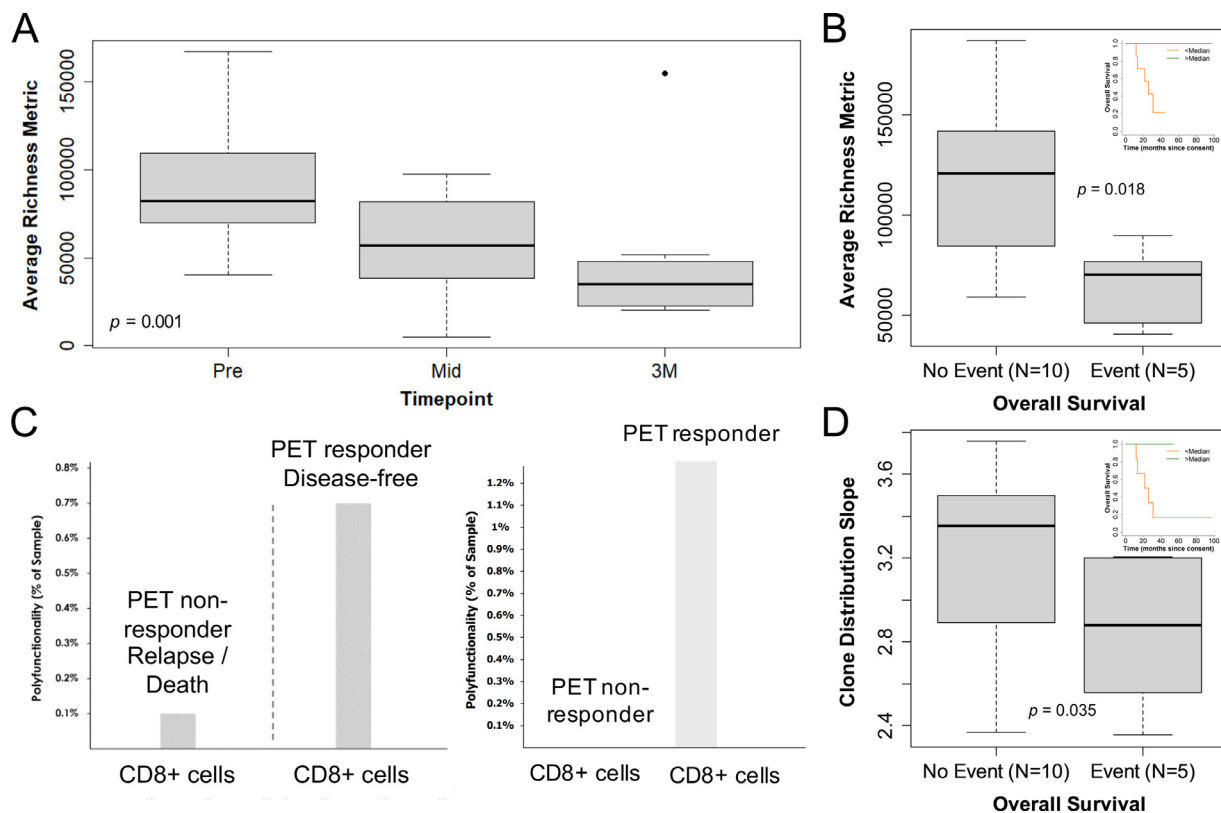

Fig. 5 T-cell receptor (TCRb CDR3) richness boxplots over pre/mid/posttreatment timepoints **(A)**, TCR richness and clone distribution slope boxplots grouped by overall survival status (no event = alive, event = deceased) with Kaplan-Meier insets **(B,D)**, and pretreatment CD8+ T-cell polyfunctionality for pairs of positron emission tomography (PET) responders and PET nonresponders **(C)**.

Discussion

We conducted a phase II trial testing selectively adaptive radiation dose escalation in patients classified as non-responders on midchemoradiation PET/computed tomography, with the objective of improving OS. All of the patients received concurrent platinum doublet chemotherapy, and approximately half of the patients received durvalumab postchemoradiation in accordance with the PACIFIC trial results that changed the standard of care for this population.[2] The focus of this manuscript is on the prognostic value of midchemoradiation FDG-PET/computed tomography, and possible associations between PET response and immunologic biomarkers. This biomarker substudy has a number of limitations, including a modest trial cohort, small sample sizes for the biomarker assays, and reduced statistical power for exploratory correlative analysis beyond the primary endpoint of the trial.

We found that total lesion glycosis on the midchemoradiation PET is associated with OS and PFS. Multiple prior series have found changes in SUV_{max} during chemoradiation to be prognostic for survival.[10] In our trial, being a PET responder versus nonresponder no longer conferred a difference in OS or PFS, perhaps due in part to our adaptive dose escalation in patients based on PET interval changes during chemoradiation, which may have mitigated the prognostic power of the PET response. However, in agreement with other published reports,[5,10,42] we found that midtreatment TLG was associated with OS and PFS, potentially serving as a marker of disease burden, even after adjustments for clinical and treatment factors. Patients classified as PET nonresponders on the midtreatment scan who also presented with a high residual TLG had the worst outcomes. This strategy could potentially help risk-stratify patients for further treatment intensification.

Our findings suggest a correlation between midtreatment PET response and PD-L1 expression, with PD-L1 positive tumors likely to be PET responders and PD-L1 negative tumors likely to be PET nonresponders. Tumor response to radiation treatment requires an intact immune system with functional T-cells,[23] and radiation has been shown to induce a proinflammatory tumor microenvironment via the induction of an immunogenic cell death.[43,44] Because PD-L1 expression plays a major role in suppressing adaptive immunity, it is possible that radiation treatment could produce a proinflammatory environment that helps overcome PD-L1 induced immune suppression.

Our analysis of germline DNA SNPs found differences in gene alteration frequency between PET responders and nonresponders, particularly in immunology pathways, which also correlated with survival. The JAK-STAT signaling pathway plays critical roles in cytokine receptors and can modulate the polarization of T helper cells. A recent report by Shahamatdar et al[45] analyzing germline variants in the TCGA cohort demonstrated that host genetics are associated with phenotypes that describe the immune component of the tumor microenvironment; they found 1 SNP associated with the amount of infiltrating follicular helper T cells and 23 candidate genes, some of which are involved in cytokine-mediated signaling. Our patient cohort supports prior findings that patients with greater TCR richness in the peripheral blood had improved survival compared with patients with less clonal richness.[46-48] TCR richness declined with chemoradiation although a smaller midtreatment decline in TCR diversity was associated with improved survival. Pretreatment TCR clone distribution slope, among other diversity metrics, was correlated with PET response status, but none of the TCR diversity metrics were correlated with midtreatment residual TLG. This suggests that PET-response status may be a marker of cancer/patient biology, but TLG is an independent measure of cancer disease burden. Single cell functional assays were performed on the peripheral blood for a small subset of patients, suggesting midtreatment PET responders had higher percentages of peripheral polyfunctional CD8+ T-cells compared with nonresponders. We also saw that select plasma cytokines are associated with OS and PFS and correlated with PET response, including TNFα, TNFR1, TGFb, and MIP1.

Although our trial population is not identical to the PACIFIC trial population (which only included patients who recovered from toxicity of chemoradiation) or to the patients in RTOG 0617 (none received durvalumab postchemoradiation),[15] our results compare favorably against both trials: our 1-year OS was 82% (vs 83.1% in PACIFIC and 80.0% in RTOG 0617), our 1-year PFS was 53% (vs 55.9% in PACIFIC and 49.2% in RTOG 0617), and our 1-year LRC was 88% (vs 83.7% in RTOG 0617, and 12.6% lung recurrence plus 6.5% nodal recurrence in PACIFIC). We saw an increase in both PFS and PNM with durvalumab, although neither were statistically significant in our modest cohort. In our trial, disease recurrence was driven primarily by distant metastatic progression, with distant metastasis being a site of first recurrence in 19/23 (83%) patients. This suggests improvement in systemic disease control is needed in a subset of patients to further improve patient outcomes.

Conclusions

Within a prospective phase 2 trial of response-adaptive radiation dose escalation for patients with unresectable NSCLC, we found in this biomarker substudy that midchemoradiation PET imaging has prognostic value for survival outcomes and that PET response status may be linked with peripheral T-cell function. The combination of PET response and peripheral blood biomarkers could

be used to guide further clinical trials of treatment intensi-fication by identifying patients at highest risk of treatment failure.

Supplementary materials

Supplementary material associated with this article can be found, in the online version, at doi:10.1016/j.adro.2021.100857.

References

1. Antonia SJ, Villegas A, Daniel D, et al. Overall survival with durva-lumab after chemoradiotherapy in stage III NSCLC. *New Engl J Med*. 2018;379:2342–2350.
2. Antonia SJ, Villegas A, Daniel D, et al. Durvalumab after chemora-diotherapy in stage III non-small-cell lung cancer. *New Engl J Med*. 2017;377:1919–1929.
3. Zeng J, Bowen SR. Treatment intensification in locally advanced/unresectable NSCLC through combined modality treatment and precision dose escalation. *Semin Radiat Oncol*. 2021;31:105–111.
4. Gray JE, Villegas A, Daniel D, et al. Three-year overall survival with durvalumab after chemoradiotherapy in stage III NSCLC-update from PACIFIC. *J Thoracic Oncol*. 2020;15:288–293.
5. Gensheimer MF, Hong JC, Chang-Halpenny C, et al. Mid-radiother-apy PET/CT for prognostication and detection of early progression in patients with stage III non-small cell lung cancer. *Radiother Oncol*. 2017;125:338–343.
6. Yossi S, Krhili S, Muratet JP, Septans AL, Campion L, Denis F. Early assessment of metabolic response by 18F-FDG PET during concom-itant radiochemotherapy of non-small cell lung carcinoma is associ-ated with survival: A retrospective single-center study. *Clin Nucl Med*. 2015;40:e215–e221.
7. Huang W, Zhou T, Ma L, et al. Standard uptake value and met-abolic tumor volume of (1)(8)F-FDG PET/CT predict short-term outcome early in the course of chemoradiotherapy in advanced non-small cell lung cancer. *Eur J Nucl Med Mol Imag*. 2011;38:1628–1635.
8. Kong FS, Li L, Wang W, et al. Greater reduction in mid-treatment FDG-PET volume may be associated with worse survival in non-small cell lung cancer. *Radiother Oncol*. 2019;132:241–249.
9. Brodin NP, Tome WA, Abraham T, Ohri N. 18)F-fluorodeoxyglu-cose PET in locally advanced non-small cell lung cancer: From pre-dicting outcomes to guiding therapy. *PET Clin*. 2020;15:55–63.
10. van Elmpt W, Ollers M, Dingemans AM, Lambin P, De Ruysscher D. Response assessment using 18F-FDG PET early in the course of radiotherapy correlates with survival in advanced-stage non-small cell lung cancer. *J Nucl Med*. 2012;53:1514–1520.
11. Kaira K, Kuji I, Kagamu H. Value of (18)F-FDG-PET to predict PD-L1 expression and outcomes of PD-1 inhibition therapy in human cancers. *Cancer Imag*. 2021;21:11.
12. Zhao L, Liu J, Wang H, Shi J. Association between (18)F-FDG meta-bolic activity and programmed death ligand-1 (PD-L1) expression using 22C3 immunohistochemistry assays in non-small cell lung cancer (NSCLC) resection specimens. *Br J Radiol*. 2021;94:20200397.
13. Ohri N, Piperdi B, Garg MK, et al. Pre-treatment FDG-PET predicts the site of in-field progression following concurrent chemoradio-therapy for stage III non-small cell lung cancer. *Lung Cancer*. 2015;87:23–27.
14. Na F, Wang J, Li C, Deng L, Xue J, Lu Y. Primary tumor standard-ized uptake value measured on F18-fluorodeoxyglucose positron emission tomography is of prediction value for survival and local control in non-small-cell lung cancer receiving radiotherapy: Meta-analysis. *J Thoracic Oncol*. 2014;9:834–842.
15. Bradley JD, Paulus R, Komaki R, et al. Standard-dose versus high-dose conformal radiotherapy with concurrent and consolidation carboplatin plus paclitaxel with or without cetuximab for patients with stage IIIA or IIIB non-small-cell lung cancer (RTOG 0617): A randomised, two-by-two factorial phase 3 study. *Lancet Oncol*. 2015;16:187–199.
16. Bradley JD, Paulus R, Graham MV, et al. Phase II trial of postopera-tive adjuvant paclitaxel/carboplatin and thoracic radiotherapy in resected stage II and IIIA non-small-cell lung cancer: Promising long-term results of the radiation therapy oncology group - RTOG 9705. *J Clin Oncol*. 2005;23:3480–3487.
17. Machtay M, Bae K, Movsas B, et al. Higher biologically effective dose of radiotherapy is associated with improved outcomes for locally advanced non-small cell lung carcinoma treated with chemo-radiation: An analysis of the Radiation Therapy Oncology Group. *Int J Radiat Oncol Biol Phys*. 2012;82:425–434.
18. Senan S, Brade A, Wang LH, et al. PROCLAIM: Randomized phase III trial of pemetrexed-cisplatin or etoposide-cisplatin plus thoracic radiation therapy followed by consolidation chemotherapy in locally advanced nonsquamous non-small-cell lung cancer. *J Clin Oncol*. 2016;34:953–962.
19. van Diessen J, De Ruysscher D, Sonke JJ, et al. The acute and late toxicity results of a randomized phase II dose-escalation trial in non-small cell lung cancer (PET-boost trial). *Radiother Oncol*. 2019;131:166–173.
20. Raman S, Bissonnette JP, Warner A, et al. Rationale and protocol for a canadian multicenter phase II randomized trial assessing selective metabolically adaptive radiation dose escalation in locally advanced non-small-cell lung cancer (NCT02788461). *Clin Lung Cancer*. 2018;19:e699–e703.
21. Kong FM, Ten Haken RK, Schipper M, et al. Effect of midtreatment PET/CT-adapted radiation therapy with concurrent chemotherapy in patients with locally advanced non-small-cell lung cancer: A phase 2 clinical trial. *JAMA Oncol*. 2017;3:1358–1365.
22. Lee E, Zeng J, Miyaoka RS, et al. Functional lung avoidance and response-adaptive escalation (FLARE) RT: Multimodality plan dosimetry of a precision radiation oncology strategy. *Med Phys*. 2017;44:3418–3429.
23. Lee Y, Auh SL, Wang Y, et al. Therapeutic effects of ablative radia-tion on local tumor require CD8+ T cells: Changing strategies for cancer treatment. *Blood*. 2009;114:589–595.
24. Das S, Sharma M, Saharia D, et al. Data in support of in vivo studies of silk based gold nano-composite conduits for functional peripheral nerve regeneration. *Data Brief*. 2015;4:315–321.
25. Aristophanous M, Penney BC, Pelizzari CA. The development and testing of a digital PET phantom for the evaluation of tumor volume segmentation techniques. *Med Phys*. 2008;35:3331–3342.
26. Werner-Wasik M, Nelson AD, Choi W, et al. What is the best way to contour lung tumors on PET scans? Multiobserver validation of a gradient-based method using a NSCLC digital PET phantom. *Int J Radiat Oncol Biol Phys*. 2012;82:1164–1171.
27. JH O, Lodge MA, Wahl RL. Practical PERCIST: A simplified guide to PET response criteria in solid tumors 1.0. *Radiology*. 2016;280:576–584.
28. Wahl RL, Jacene H, Kasamon Y, Lodge MA. From RECIST to PER-CIST: Evolving considerations for PET response criteria in solid tumors. *J Nucl Med*. 2009;50(Suppl 1):122S–150S.
29. Simpson EH. Measurement of diversity. *Nature*. 1949;163:688.
30. Zhang Y, Kim TJ, Wroblewska JA, et al. Type 3 innate lymphoid cell-derived lymphotoxin prevents microbiota-dependent inflamma-tion. *Cell Mol Immunol*. 2018;15:697–709.
31. Smith GL, Ganz PA, Bekelman JE, et al. Promoting the appropriate use of advanced radiation technologies in oncology: Summary of a National Cancer Policy Forum workshop. *Int J Radiat Oncol Biol Phys*. 2017;97:450–461.

32. Rolle CE, Tan YC, Seiwert TY, et al. Expression and mutational analysis of c-CBL and its relationship to the MET receptor in head and neck squamous cell carcinoma. *Oncotarget*. 2017;8:18726–18734.

33. Daillere R, Vetizou M, Waldschmitt N, et al. *Enterococcus hirae* and *Barnesiella intestinihominis* facilitate cyclophosphamide-induced therapeutic immunomodulatory effects. *Immunity*. 2016;45:931–943.

34. Busser B, Lupo J, Sancey L, et al. Plasma circulating tumor DNA levels for the monitoring of melanoma patients: Landscape of available technologies and clinical applications. *BioMed Res Int*. 2017;2017: 5986129.

35. Das SK, Chakraborty S, Ramakrishnan R. Critical benchmarking of popular composite thermochemistry models and density functional approximations on a probabilistically pruned benchmark dataset of formation enthalpies. *J Chem Phys*. 2021;154: 044113.

36. Das S, Scholes HM, Sen N, Orengo C. CATH functional families predict functional sites in proteins. *Bioinformatics*. 2021;23:1099–1106.

37. Chiu CH, Wang YT, Walther BA, Chao A. An improved nonparametric lower bound of species richness via a modified good-turing frequency formula. *Biometrics*. 2014;70:671–682.

38. Efron B, Thisted R. Estimating the number of unseen species: How many words did Shakespeare know? *Biometrika*. 1976;63:435–447.

39. Daley T, Smith AD. Predicting the molecular complexity of sequencing libraries. *Nat Methods*. 2013;10:325–327.

40. Pielou EC. The measurement of diversity in different types of biological collections. *J Theoret Biol*. 1966;13:131–144.

41. DeWolf S, Grinshpun B, Savage T, et al. Quantifying size and diversity of the human T cell alloresponse. *JCI Insight*. 2018;3.

42. Chen HHW, Su WC, Guo HR, Lee BF, Chiu NT. Prognostic value of volumetric metabolic parameter changes determined by during and after radiotherapy-based (18) F-FDG PET/CT in stage III non-small cell lung cancer. *Kaohsiung J Med Sci*. 2019;35:151–159.

43. Weichselbaum RR, Liang H, Deng L, Fu YX. Radiotherapy and immunotherapy: A beneficial liaison? *Nat Rev Clin Oncol*. 2017;14:365–379.

44. Golden EB, Apetoh L. Radiotherapy and immunogenic cell death. *Semin Radiat Oncol*. 2015;25:11–17.

45. Shahamatdar S, He MX, Reyna MA, et al. Germline features associated with immune infiltration in solid tumors. *Cell Rep*. 2020;30:2900–2908. e4.

46. Kansy BA, Shayan G, Jie HB, et al. T cell receptor richness in peripheral blood increases after cetuximab therapy and correlates with therapeutic response. *Oncoimmunology*. 2018;7: e1494112.

47. Postow MA, Manuel M, Wong P, et al. Peripheral T cell receptor diversity is associated with clinical outcomes following ipilimumab treatment in metastatic melanoma. *J Immunother Cancer*. 2015;3:23.

48. Charles J, Mouret S, Challende I, et al. T-cell receptor diversity as a prognostic biomarker in melanoma patients. *Pigment Cell Melanom Res*. 2020;33:612–624.